

## Longitudinal spin structure of the nucleon at COMPASS

---

**Yann Bedfer**<sup>\*†</sup>

*Irfu/DphN CEA Saclay, France*

*E-mail: [Yann.Bedfer@cern.ch](mailto:Yann.Bedfer@cern.ch)*

For a large fraction of its already twenty year long existence, the COMPASS collaboration has studied the polarised structure of the nucleon via muon-nucleon scattering. This paper summarizes the final results obtained in longitudinally polarised DIS, either inclusive or semi-inclusive. For inclusive DIS, these cover the measurements of structure function  $g_1$ , and the information extracted from them in terms of polarised PDFs (pPDFs) and Bjorken sum rule. From  $g_1$  measurements alone, combining COMPASS with world data, the quark spin contribution to the nucleon spin is determined to be  $0.26 < \Delta\Sigma < 0.36$ . And from COMPASS data alone, the Bjorken sum rule is verified to 9% accuracy. In semi-inclusive DIS, more information can be gained on the pPDFs of sea quarks and gluons. A selection of our achievements along this line are reported.

*23rd International Spin Physics Symposium - SPIN2018 -  
10-14 September, 2018  
Ferrara, Italy*

---

<sup>\*</sup>Speaker.

<sup>†</sup>On behalf of the COMPASS collaboration.

## 1. Introduction

Polarised aspects of the nucleon structure are still less known than unpolarised ones. COMPASS is one of the several experiments set up to gain further insight into this polarised structure over the last twenty years. It fulfils its specifications by measuring double spin cross-section asymmetries in lepton-nucleon scattering using muons of energy between 160 and 200 GeV.

The experiment is a fixed target magnetic spectrometer. It is described in details in [1] and [2]. As far as polarised nucleon structure is concerned, it operates in conjunction with two other equally important pieces of equipment: a polarised muon beam and a polarised target, which fulfil the requisites of double spin measurements. The muon beam delivered leptons with a natural, and hence stable, longitudinal polarisation of  $\sim 80\%$  and an intensity of about  $5 \times 10^7$  per second. The polarised target was designed with an impressive 1.2 m of length, compensating the weakness of the beam intensity. It provided protons and deuterons polarised to  $\sim 90\%$  and  $\sim 50\%$ , respectively. It was subdivided into cells arranged along the beam axis and polarised in opposite direction, allowing a simultaneous recording of the two nucleon spin states. The polarisation configuration was regularly inverted.

The cross-section asymmetry  $A_{LL}$  is extracted from the difference in number of interactions for parallel and anti-parallel spins of muon and nucleon. For inclusive measurements, this asymmetry when divided by the depolarisation factor is approximately equal to  $A_1$ . The latter, together with the knowledge of the unpolarised structure function  $F_2$  and the ratio  $R$ , give the spin-dependent structure function  $g_1$ . Parametrisations of  $F_2$  and  $R$  were taken from Refs [3] and [4], respectively.

## 2. Results for $A_1^p$ and $g_1^p$

Results presented here, Fig. 1, are based on data collected in 2007 [5] and 2011 [6]. In 2011 the beam energy was increased to 200 GeV to access higher values of  $Q^2$  and lower values of  $x$ .

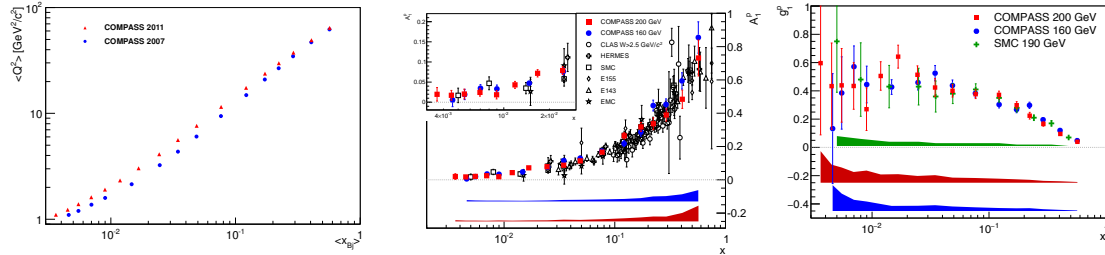


**Figure 1:** COMPASS results for  $A_1^p$  and  $g_1^p$  at 160 [5] and 200 GeV [6]. **Left:** mean value of  $Q^2$  vs.  $x$ . **Middle:**  $A_1^p$  vs.  $x$ , compared to the other world data (EMC [7], CLAS [8], HERMES [9], E143 [10], E155 [11] and SMC [3]). **Right:**  $g_1^p$  vs.  $x$  at measured values of  $Q^2$ , compared to the SMC measurements [3]. Bands at the bottom indicate the systematic uncertainties of the COMPASS data at 160 GeV (blue), 200 GeV (red) and SMC at 190 GeV (green).

Results on  $A_1^p$  and  $g_1^p$  for the two energies agree very well with each other and with the world data, Fig. 1, thus illustrating their weak dependence on  $Q^2$ . The strong point of COMPASS is that it reaches down to low values of Bjorken  $x$ , viz.  $3.5 \cdot 10^{-3}$ . A very interesting fact is that  $g_1^p(x)$  stays finite and positive down to these low values.

### 3. Results for $A_1^d$ and $g_1^d$

Results presented here, Fig. 2, are based on data collected in 2002-2004 [12] and 2006 [13]. Results on  $A_1^d$  and  $g_1^d$  from both samples agree very well with each other and with the world data, Fig. 2, thus illustrating their weak dependence on  $Q^2$ . Contrary to the behaviour of  $g_1^p$  and to the hints from SMC [3],  $g_1^d$  is compatible with zero at lowest measured  $x$ .

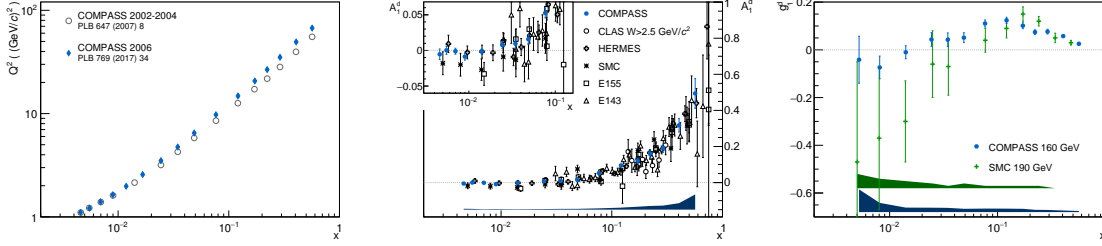


**Figure 2:** COMPASS results for  $A_1^d$  and  $g_1^d$  for the data collected in 2002-2004 [12] and 2006 [13]. **Left:** mean values of  $Q^2$  vs.  $x$ . **Middle:**  $A_1^d$  vs.  $x$ , compared to the other world data (CLAS [8], HERMES [9], SMC [3], E143 [10] and E155 [14]). **Right:**  $g_1^d$  vs.  $x$  for both samples combined and at measured values of  $Q^2$  compared to the SMC measurements [3]. Bands at the bottom indicate the systematic uncertainties of the COMPASS data (blue) and SMC (green).

### 4. NLO QCD fit of pPDFs to $g_1$ world data

The COMPASS results are used in an NLO QCD fit, together with the world data on  $g_1^p$ ,  $g_1^d$  and  $g_1^{3\text{He}}$  with  $Q^2 > 1 \text{ GeV}^2$  and  $W^2 > 10 \text{ GeV}^2$  [6, 13]. Renormalisation/factorisation scheme is  $\overline{\text{MS}}$ . Fitted are the gluon distribution  $\Delta g$ , the singlet  $\Delta q^S = \Delta(u + \bar{u}) + \Delta(d + \bar{d}) + \Delta(s + \bar{s})$  and two non-singlet quark distributions  $\Delta q_3 = \Delta(u + \bar{u}) - \Delta(d + \bar{d})$  and  $\Delta q_8 = \Delta(u + \bar{u}) + \Delta(d + \bar{d}) - 2\Delta(s + \bar{s})$ . The functional shape at input scale  $Q_0^2$  is:

$$\Delta f_k(x) = \eta_k x^{\alpha_k} (1-x)^{\beta_k} (1 + \gamma_k x) / \int_0^1 x^{\alpha_k} (1-x)^{\beta_k} (1 + \gamma_k x) dx ,$$

where  $k = S, 3, 8, g$  and  $\eta_k$  is the first moment of  $\Delta f_k(x)$  at  $Q_0^2$ . But several simplifications are applied, leaving a maximum of 11 free parameters:  $\gamma_g = \gamma_3 = \gamma_8 = 0$ , and  $\beta_g$  is fixed at the value of the unpolarised distribution in the MSTW PDF set [15]. In addition, the non-singlet moments are fixed by the baryon decay constants:  $\eta_3 = F + D$ ,  $\eta_8 = 3F - D$ , assuming SU(2) and SU(3) symmetries. The positivity constraint on  $q + \bar{q}$  and  $g$  is enforced by a  $\chi^2$  penalty. Only statistical errors are considered in the fit; normalisations of data sets are allowed to vary, constrained by systematical uncertainties. Varying the input scale allows to generate sets of solutions. Doing this while fixing parameter  $\gamma_S$  to zero or not, generates two such sets, all elements of which describe the data equally well. Their envelope represents the systematical uncertainty.

Results of the fit are shown in Fig. 3. The contribution of quark spin to the nucleon spin  $\Delta\Sigma$  is found to be:

$$\Delta\Sigma = 0.31 \pm 0.05 ,$$

while the gluon distribution  $\Delta g$  turns out to be largely undetermined by inclusive measurements.

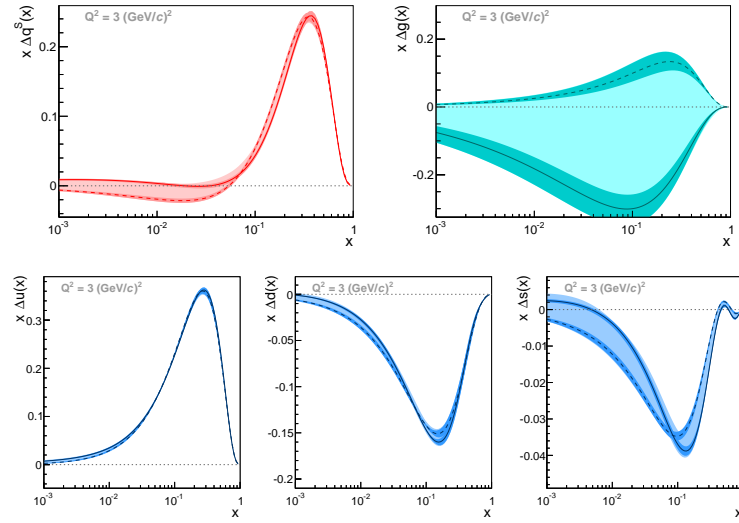


**Figure 3:** Results of the QCD fit to  $g_1$  world data, at  $Q^2 = 3 \text{ GeV}^2$  for two sets of solutions [6], see text. Top: singlet  $x\Delta q^S(x)$  and gluon distribution  $x\Delta g(x)$ . Bottom: distributions of  $x[\Delta q(x) + \Delta \bar{q}(x)]$  for  $u$ ,  $d$  and  $s$  flavours. Continuous and dashed lines correspond to the fits with  $Q_0^2 = 1 \text{ GeV}^2$ . The dark bands represent statistical uncertainties. The light bands, overlaying the dark ones, represent systematic uncertainties.

## 5. First moment of structure function $g_1^{\text{NS}}$ and Bjorken sum rule

The structure function,  $g_1^{\text{NS}}$  is defined as:  $g_1^{\text{NS}} = g_1^{\text{p}} - g_1^{\text{n}} = 2[g_1^{\text{p}} - g_1^{\text{d}}/(1 - 1.5\omega_D)]$ , where  $\omega_D = 0.05 \pm 0.02$  is the contribution of the D-state in the deuteron. Its first moment is the right hand side of the fundamental Bjorken sum rule. The extraction of the  $\Gamma_1^{\text{NS}}$  from COMPASS data alone, integrated over  $x$  and extrapolated into the high  $x$  region, gives:

$$\Gamma_1^{\text{NS}} = 0.192 \pm 0.007_{\text{stat.}} \pm 0.0015_{\text{syst.}}$$

which leads to a validation of the sum rule at the level of 9%, see Ref. [13] for the details.

## 6. Semi-inclusive asymmetries $A_1^\pi$ and $A_1^K$

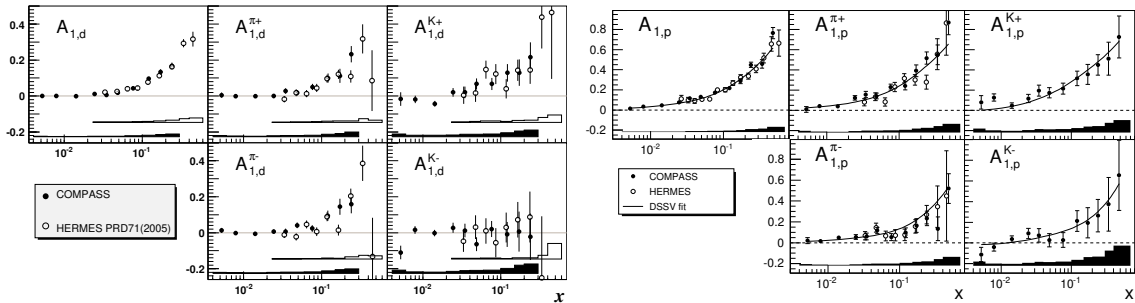


**Figure 4:** COMPASS results for  $A_1$  and  $A_1^h$ ,  $h = \pi^\pm, K^\pm$  on polarised  $d$  [16] and  $p$  [17] targets, compared with HERMES data [9, 18]. Bands at the bottom indicate the systematic uncertainties of the COMPASS (full bands) and HERMES (empty bands) data.

Additional information can be obtained from SIDIS data, *viz.* the double-spin asymmetries for single inclusive production of pions and kaons,  $A_1^h$ , with  $h = \pi^\pm, K^\pm$ . When determined for both polarised  $p$  and  $d$  targets and combined with inclusive data, they constitute a complete set allowing for the extraction of fully flavour and charge separated pPDFs. COMPASS measured these asymmetries [16, 17], see Fig. 4, and determined fully separated pPDFs from a LO analysis of its own inclusive and SIDIS data set [17]. A better determination of pPDFs is obtained from global QCD fits at NLO, combining DIS and SIDIS data, such as LSS [19], and also polarised  $pp$  data from RHIC, such as DSSV [20] and NNPDF [21]. SIDIS data, and in particular COMPASS, play an essential role there, in the charge and flavour separation. They give some indications on such issues as the breaking of SU(3) symmetry, the strangeness distribution, polarised and unpolarised, and the flavour asymmetry of the polarised sea. For the latter, data favour  $\Delta\bar{u} > 0$ ,  $\Delta\bar{d} < 0$ , as is expected from naive considerations based on the Pauli principle and is predicted by a number of quark models [22]. These indications are still affected by large uncertainties, though. Complementary information along these lines will come from precise measurements of  $W^\pm$  production at RHIC.

However the inclusion of SIDIS data in the determination of pPDFs introduces a dependence upon the hadronisation process, which is described in pQCD by parton-to-hadron fragmentation functions (FFs). In order to exploit the full potential of SIDIS data, and clarify the above-mentioned flavour symmetry issues, several phenomenology groups are starting to perform simultaneous QCD fits of PDFs, polarised and unpolarised, and FFs, combining data from DIS,  $pp$  collisions and  $e^+e^-$  annihilations [23, 24]. COMPASS provides unpolarised hadron multiplicities [25, 26], in addition to double-spin asymmetries, as inputs to these fits.

## 7. Direct measurement of $\Delta g$

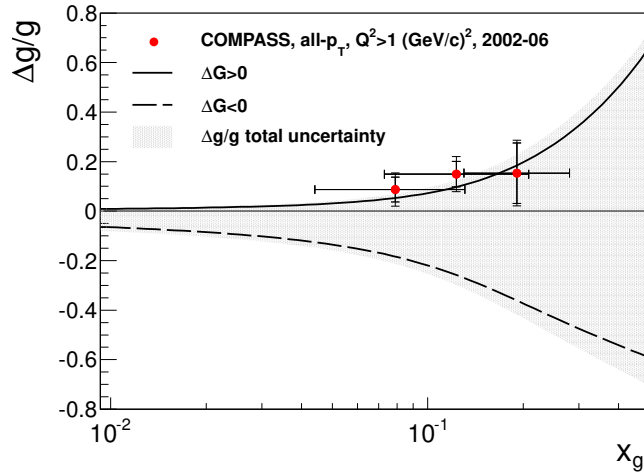


**Figure 5:**  $\Delta g/g$  vs.  $x$ : LO analysis of COMPASS DIS data [27] in three ranges of  $x_g$  compared to predictions from COMPASS NLO QCD fit [6] at  $Q^2 = 3 \text{ GeV}^2$ . The three data points are not fully independent. Horizontal bars represent  $1\sigma$  confidence intervals. Inner error bars represent statistical uncertainties and outer ones statistical and systematic uncertainties combined in quadrature.

COMPASS has also explored several avenues to better constrain the gluon polarised PDF,  $\Delta g$ . One of these is the semi-inclusive single-hadron production as a function of  $p_T$ ,  $p_T$  being the hadron transverse momentum with respect to the virtual photon.

A re-analysis [27] was performed on the data with  $Q^2 > 1 \text{ GeV}^2$  taken on polarised deuterons. It uses a novel method, putting the data to better use. It yields:

$$\langle \Delta g/g \rangle = 0.113 \pm 0.038_{(stat.)} \pm 0.036_{(syst.)}$$

for a weighted average of gluon momentum fraction  $\langle x_g \rangle \approx 0.10$  and an average  $Q^2$  of  $3 \text{ GeV}^2$ . This result is compatible with and supersedes our previous result [28] obtained from the same  $Q^2 > 1 \text{ GeV}^2$  data. It favours a positive gluon polarisation in the measured  $x_g$  range. The gluon polarisation is also extracted in three bins which correspond to three partially overlapping  $x_g$  ranges. These are shown in Fig. 5. Within experimental uncertainties, the values do not show any significant dependence on  $x_g$ .

The above analysis relies on a Monte Carlo generator, *viz.* LEPTO [29], to go from the hadron to the parton level. And at parton level, it performs calculations at order  $\mathcal{O}(\alpha_S)$ , *i.e.* LO for the gluon-induced subprocesses. For this reason, we consider our approach to be a LO analysis, although LEPTO is not strictly speaking a fixed-order pQCD program. This is a strong limitation, given that state-of-the-art QCD fits of polarised PDFs are now based on NLO pQCD calculations. Remains that the results demonstrate the potential of COMPASS single-hadron production data to constrain  $\Delta g$ . These are made available in Ref. [28], in the shape of raw double spin asymmetries in bins of  $p_T$ .

Single-hadron production at high  $p_T$  was also measured by COMPASS in the low  $Q^2$  quasi-real photoproduction region [30]. This time, a pQCD framework that was developed up to NLO is available to interpret the data [31]. Provided a technique known as "threshold resummation" at next-to-leading logarithm (NLL) is applied, the calculations reproduce COMPASS unpolarised cross-section measurements [32] within theoretical uncertainties. This hence demonstrates the applicability of the framework to our kinematical domain. The resummation technique has recently been extended to the polarised case [33] and applied to the COMPASS case. Results show improved agreement with polarised PDFs from DSSV++ [20], but the interpretation of the data is still affected by uncertainties arising from fragmentation functions.

## 8. Conclusions

Results presented in this paper constitute the COMPASS legacy on longitudinally polarised inclusive DIS and SIDIS measurements for the determination of  $p_T$ -integrated polarised PDFs (pPDFs). Inclusive and single-hadron double-spin asymmetries have been included in global QCD fits of pPDFs. Direct measurements of the gluon distribution *via* single-hadron production at high  $p_T$ , although not included in global fits, show promising results.

More results concerning the azimuthal modulation of single and double-spin asymmetries are becoming available [34] and await publications.

## References

- [1] COMPASS Collaboration, P. Abbon *et al.*, Nucl. Instrum. Meth. A **577** (2007) 455.

- [2] COMPASS Collaboration, P. Abbon *et al.*, Nucl. Instrum. Meth. A **779** (2015) 69.
- [3] SMC Collaboration, B. Adeva *et al.*, Phys. Rev. D **58** (1998) 112001.
- [4] E143 Collaboration, K. Abe *et al.* Phys. Lett. B **452** (1999) 194
- [5] COMPASS Collaboration, M.G. Alekseev, *et al.*, Phys. Lett. B **690** (2010) 466.
- [6] COMPASS Collaboration, C. Adolf, *et al.*, Phys. Lett. B **753** (2016) 18.
- [7] EM Collaboration, J. Ashman *et al.*, Phys. Lett. B **206** (1988) 364; Nucl. Phys. B **328** (1989) 1.
- [8] CLAS Collaboration, K. V. Dharmawardane *et al.*, Phys. Lett. B **641** (2006) 11.
- [9] HERMES Collaboration, A. Airapetian *et al.*, Phys. Rev. D **75** (2007) 012007
- [10] E143 Collaboration, K. Abe *et al.*, Phys. Rev. D **58** (1998) 112003.
- [11] E155 Collaboration, P.L. Anthony *et al.*, Phys. Lett. B **493** (2000) 19.
- [12] COMPASS Collaboration, V.Yu. Alexakhin *et al.*, Phys. Lett. B **647** (2007) 8.
- [13] COMPASS Collaboration, C. Adolph *et al.*, Phys. Lett. B **769** (2017) 34.
- [14] E155 Collaboration, P. L. Anthony, et al., Phys. Lett. B **463** (1999) 339.
- [15] MSTW, A.D. Martin *et al.*, Eur. Phys. J. C **63** (2009) 189.
- [16] COMPASS Collaboration, M. Alekseev *et al.*, Phys. Lett. B **680** (2009) 217
- [17] COMPASS Collaboration, M. G. Alekseev *et al.*, Phys. Lett. B **693** (2010) 227
- [18] HERMES Collaboration, A. Airapetian *et al.*, Phys. Rev. D **71** (2005) 012003
- [19] E. Leader, A. V. Sidorov and D. B. Stamenov, J. Phys. Conf. Ser. **295** (2011) 012054.
- [20] D. de Florian, R. Sassot, M. Stratmann and W. Vogelsang, Phys. Rev. Lett. **113** (2014) no.1, 012001
- [21] NNPDF Collaboration, E. R. Nocera *et al.*, Nucl. Phys. B **887** (2014) 276
- [22] D. de Florian, R. Sassot, M. Stratmann and W. Vogelsang, Phys. Rev. D **80** (2009) 034030
- [23] J. J. Ethier, N. Sato and W. Melnitchouk, Phys. Rev. Lett. **119** (2017) no.13, 132001
- [24] I. Borsa, R. Sassot and M. Stratmann, Phys. Rev. D **96** (2017) no.9, 094020
- [25] COMPASS Collaboration, C. Adolph *et al.* Phys. Lett. B **767** (2017) 133
- [26] COMPASS Collaboration, C. Adolph *et al.* Phys. Lett. B **764** (2017) 1
- [27] COMPASS Collaboration, C. Adolph *et al.*, Eur. Phys. J. C **77** (2017) no.4, 209
- [28] COMPASS Collaboration, C. Adolph *et al.*, Phys. Lett. B **718** (2013) 922
- [29] G. Ingelman, A. Edin and J. Rathsmann, Comput. Phys. Commun. **101** (1997) 108.
- [30] COMPASS Collaboration, C. Adolph *et al.*, Phys. Lett. B **753** (2016) 573
- [31] B. Jäger, M. Stratmann and W. Vogelsang, Eur. Phys. J. C **44** (2005) 533
- [32] COMPASS Collaboration, C. Adolph *et al.*, Phys. Rev. D **88** (2013) no.9, 091101
- [33] C. Uebler, A. Schäfer and W. Vogelsang, Phys. Rev. D **96** (2017) no.7, 074026
- [34] B. Parsamyan, PoS DIS **2017** (2018) 259